

Article

Heterogeneous Photo-Fenton Catalytic Degradation of Practical Pharmaceutical Wastewater by Modified Attapulgite Supported Multi-Metal Oxides

Manjing Lu ¹, Jiaqi Wang ¹, Yuzhong Wang ¹ and Zhengguang He ^{2,*}

¹ School of Water Conservancy Science & Engineering, Zhengzhou University, Zhengzhou 450000, China; lumanjing@gs.zzu.edu.cn (M.L.); wangjiaqi@gs.zzu.edu.cn (J.W.); wangyuzhong@gs.zzu.edu.cn (Y.W.)

² School of Ecology and Environment, Zhengzhou University, Zhengzhou 450000, China

* Correspondence: hezhengguang@zzu.edu.cn; Tel.: +86-138-3817-2129

Abstract: Chemical synthetic pharmaceutical wastewater has characteristics of high concentration, high toxicity and poor biodegradability, so it is difficult to directly biodegrade. We used acid modified attapulgite (ATP) supported Fe-Mn-Cu polymetallic oxide as catalyst for multi-phase Fenton-like ultraviolet photocatalytic oxidation (photo-Fenton) treatment with actual chemical synthetic pharmaceutical wastewater as the treatment object. The results showed that at the initial pH of 2.0, light distance of 20 cm, and catalyst dosage and hydrogen peroxide concentration of 10.0 g/L and 0.5 mol/L respectively, the COD removal rate of wastewater reached 65% and BOD₅/COD increased to 0.387 when the reaction lasted for 180 min. The results of gas chromatography-mass spectrometry (GC-MS) indicated that Fenton-like reaction with Fe-Mn-Cu@ATP had good catalytic potential and significant synergistic effect, and could remove almost all heterocycle compounds well. 3D-EEM (3D electron microscope) fluorescence spectra showed that the fluorescence intensity decreased significantly during catalytic degradation, and the UV humus-like and fulvic acid were effectively removed. The degradation efficiency of the nanocomposite only decreased by 5.8% after repeated use for 6 cycles. It seems appropriate to use this process as a pre-treatment for actual pharmaceutical wastewater to facilitate further biological treatment.

Keywords: pharmaceutical wastewater; heterogeneous catalyst; photo-Fenton; Fe-Mn-Cu@ATP



Citation: Lu, M.; Wang, J.; Wang, Y.; He, Z. Heterogeneous Photo-Fenton Catalytic Degradation of Practical Pharmaceutical Wastewater by Modified Attapulgite Supported Multi-Metal Oxides. *Water* **2021**, *13*, 156. <https://doi.org/10.3390/w13020156>

Received: 14 December 2020

Accepted: 6 January 2021

Published: 11 January 2021

Publisher's Note: MDPI stays neutral with regard to jurisdictional claims in published maps and institutional affiliations.



Copyright: © 2021 by the authors. Licensee MDPI, Basel, Switzerland. This article is an open access article distributed under the terms and conditions of the Creative Commons Attribution (CC BY) license (<https://creativecommons.org/licenses/by/4.0/>).

1. Introduction

With the rapid development of the pharmaceutical industry, the scale of synthetic pharmaceutical production is expanding, resulting in a large increase in the amount of wastewater generated [1]. The public faces an environmental problem of complex pharmaceutical wastewater components, which causes them to worry about the ecological environmental damage [2]. In recent years, due to the variation in raw materials and production processes of different drugs, the composition of wastewater has varied widely from location to location, which brings certain difficulties to wastewater treatment, which is also an important reason for pharmaceutical industry wastewater treatment efficiency [3]. Therefore, combined with the actual situation of chemical synthetic pharmaceutical wastewater (hereinafter referred to as chemical pharmaceutical wastewater), the type and characteristics of wastewater should be studied in depth, and wastewater treatment technology should be continuously improved to meet the development needs of the chemical synthetic pharmaceutical industry [4]. Chemical pharmaceutical wastewater mainly includes process wastewater, washing wastewater and recovery residual liquid. Due to its long production process and the low utilization rate of raw materials, the chemical composition of the wastewater is complex, with high concentration of organic matter, strong toxicity, poor biodegradability and great impact on biochemical treatment. At present, the difficulty of chemical and pharmaceutical wastewater treatment lies in reducing pollutant concentration and improving biodegradability. Traditional treatment technologies,

such as adsorption, coagulation and biological treatment, are mainly used, but there are some application problems, such as poor treatment efficiency, high cost, and easy to cause secondary pollution [5]. Moreover, the highly toxic and recalcitrant substances in the wastewater make biochemical treatment difficult to be directly applied. Therefore, an economical, effective and eco-friendly technology is needed to mineralize these pollutants into substances that are non-toxic or less toxic.

As an emerging wastewater treatment method, advanced oxidation technology has attracted the attention of many experts and scholars in recent years, among which methods heterogeneous photo-Fenton catalysis technology has been successfully applied to the treatment of refractory organic wastewater [6]. Both homogeneous Fenton and Fenton-like methods can effectively degrade refractory organic compounds in water, but they have some disadvantages, such as the release of large amounts of iron ions in water, increased chromaticity, heavy mud production, and unrecyclable catalysts. Relevant researchers have researched heterogeneous Fenton-like oxidation technology based on solid catalysts [7]. In recent years, as a green, economical and convenient catalytic method, heterogeneous photo-Fenton catalytic oxidation has been widely investigated [8,9]. The commonly used oxidants and catalysts in the treatment of chemical pharmaceutical wastewater by photo-Fenton catalytic oxidation are H_2O_2 , TiO_2 and their composites, and other metal composite materials [10–12]. Transition metals and their compound catalysts mainly refer to the catalysts formed by transition metal elements and their oxides, as well as the composite oxides between them [13]. The commonly used transition metals mainly include Fe, Mn, Cu, Co, Ni, Zn, etc. Because of its high catalytic performance in the oxidation of organic pollutants in aqueous solution, metal nano-oxide has attracted the attention of many researchers [14,15]. In recent years, it has been reported that it is feasible to treat organic pollutants with transition metal oxide as catalyst [15,16]. The application of active metal-supported multiphase catalysts can not only reduce ion leaching, but also expand the pH range and improve reusability. In addition, the application of nano-oxide in photocatalytic oxidation can degrade many tolerant organic pollutants. Moreover, the combined action of poly-metals causes heterogeneous catalysts with multiple active centers to have better catalytic activity. Li prepared an $\text{Fe}_3\text{O}_4/\text{CeO}_2$ composite material by impregnation roasting method, which played the dual role of highly efficient adsorbent and Fenton-like catalyst for organic dyes [17]. Jauhar used the sol-gel method to prepare nano-cobalt-manganese composite iron oxide and applied it to the degradation of dyes, and finally achieved good treatment effects [18]. Su prepared nanometer $\text{Fe}_x\text{Mn}_y\text{Cu}_z\text{O}_w/\gamma\text{-Al}_2\text{O}_3$ catalyst by wet impregnation and calcination, and box-Behnken studied the degradation of PVA in aqueous solution [19]. Relevant articles indicate that polymetallic catalysts have been successfully used in photo-Fenton treatment of organic pollutants [20].

Because the metal nanoparticles are easy to agglomerate, the active surface area of the catalyst is small. In order to improve their dispersibility, a mature method is to combine catalyst nanoparticles with adsorbents. Polymetallic nanoparticles are fixed to solid carriers during the synthesis process, such as activated carbon, mineral materials, carbon nanotubes and mesoporous materials [21–23]. Attapulgite, as a kind of natural mineral clay, not only has large reserves and high crystal level, but also is easy to be mined in China with obvious quality advantages [24]. Therefore, it is of great industrial application value to develop and study this kind of cheap clay resource ore and to prepare attapulgite products with large specific surface area. In addition, having a large specific surface area gives attapulgite good colloidal properties such as easy decolorization and easy adsorption. Zhang prepared an attapulgite supported Fe_2O_3 catalyst and studied its decolorization effect on dyes in heterogeneous Fenton reaction [25].

The focus of this study is to prepare multiphase $\text{Fe}_2\text{O}_3\text{-MnO-CuO}$ composite material loaded on modified ATP (labeled as Fe-Mn-Cu@ATP), and study catalytic performance in degradation of organic pollutants under different conditions by using H_2O_2 and UV irradiation in actual chemical pharmaceutical wastewater. Sodium pyrophosphate was selected as the dispersant in the purification process of ATP, and the purified ATP was modified by

acidification [26], so that the final catalyst had high reaction activity, high stability and high degradation rate [27]. Then the effects of pH, solid catalyst, hydrogen peroxide dosage and light intensity on the removal of pollutants were systematically investigated. The change rules and removal characteristics of organic compounds in wastewater before and after the reaction were revealed by GC-MS and 3D-EEM fluorescence spectra, and the reaction mechanism was further analyzed to evaluate the actual effect of photo-Fenton oxidation pretreatment. Finally, decolorization, degradation of refractory organics and improvement of biodegradability of effluent were achieved.

2. Materials and Methods

2.1. Characteristics of Pharmaceutical Wastewater

The wastewater used in the study was raw water from a pharmaceutical company in Zhengzhou, China, producing chemical API, mainly including sulfa-medrazine sodium and doxycycline hydrochloride. Table 1 describes the characteristics of the chemical pharmaceutical wastewater used in the experiment.

Table 1. Characteristics of the chemical pharmaceutical wastewater.

Parameter	Unit	Concentration
pH	-	1.0 ± 0.1
COD	mg/L	18,585 ± 265
BOD ₅	mg/L	3350 ± 150
BOD ₅ /COD	-	0.179 ± 0.015
NH ₃ -N	mg/L	1554.9 ± 17.3
TN	mg/L	1780 ± 25
NO ₃ -N	mg/L	88.5 ± 9
NO ₂ -N	mg/L	10.2 ± 0.8

Note: Data presented are mean ± standard error.

2.2. Preparation of the Catalyst

Fe-Mn-Cu@ATP was prepared by a new aeration-coprecipitation method [28]. The experimental steps in this process are as follows. The first step is to purify and modify ATP. ATP ore powder was mixed with deionized water in a certain proportion in a 1000 mL container, and sodium metaphosphate dispersant was added at a proportion of 3%. After being dispersed by oscillatory ultrasonic, it was centrifugally dried and ground into powder. Then, 10 g of purified ATP was added into 100 mL hydrochloric acid solution with 6 mol/L, stirred at 75 °C for 3 h, washed to neutral and dried. In the second step, Fe³⁺, Mn²⁺ and Cu²⁺ with molar ratio of 1:1:2 were freshly prepared and combined in the presence of excess oxygen (according to the analysis and comparison of the previous test). To this end, 2.303 g anhydrous ferric sulfate (FeSO₄), 1.946 g manganese sulfate (MnSO₄•H₂O) and 5.751 g copper sulfate (CuSO₄•5H₂O) were dissolved in 100 mL deionized water, respectively. In the next step, 10 g ATP after purified acidification was added to a large flask containing 100 mL distilled water under stirring conditions, and the three solutions were then mixed in a flask at a temperature of 70 °C at a stirring speed of 50 rpm. It was inflated in these conditions for 30 min. Then 10% ammonia was added at a very low rate (0.7 mL/min) to make the pH of the solution above 9, and the solution was mixed at a mixing rate of 50 rpm for 4 h. The solution was then placed at rest until it was completely deposited, and the resulting nanocomposite precipitated out. Finally, the formed products were centrifuged at 3000 rpm for 10 min, washed four times with deionized water and ethanol twice, washed, dried, and activated in a muff furnace at 400 °C for 3 h to reach constant weight. Fe-Mn-Cu was also prepared by the new aeration-coprecipitation method. The production process is the same as the previous steps 2 to 4, without adding carrier ATP. Afterwards, the prepared catalysts were collected separately and stored in a desiccator at room temperature. The above chemicals were obtained from commercial sources and were of analytical purity.

2.3. The Experimental Methods

Photo-Fenton catalytic degradation of chemical pharmaceutical wastewater was carried out in a self-made transparent plexiglass reactor with an effective volume of 1 L (360 mm in length, 85 mm in width, 40 mm in height and 3 mm in wall thickness). Three groups of experiments were conducted in parallel. First, 500 mL pharmaceutical wastewater was added into the reactor, where pH adjusted the pharmaceutical wastewater to 3.0 by adding 1.0 mol/L NaOH or H₂SO₄. Then a certain amount of solid catalyst (Fe-Mn-Cu@ATP) and hydrogen peroxide solution were added in turn. After the degradation reaction was started, the UV lamp was turned on with a 40 W UV lamp as the light source, the light distance was adjusted, and sampling was conducted regularly. The reaction temperature was maintained at 25 °C. The initial pH value (1–10), Fe-Mn-Cu@ATP dosage (1–12 g/L), hydrogen peroxide dosage (0.1–0.6 mol/L) and light distance were continuously studied. Photo-Fenton catalytic degradation was studied by measuring COD and other data changes of the samples. COD removal rate was determined by Equation (1):

$$\text{COD removal(\%)} = (\text{COD}_0 - \text{COD}_t) / \text{COD}_0 \times 100, \quad (1)$$

where COD₀ and COD_t are the initial and residual COD concentrations at 0 and t min, respectively.

2.4. Analytical Methods

The structure and morphology characteristics of the composite catalyst (Fe-Mn-Cu@ATP) were characterized by using a Regulus 8100 SEM (HITACHI, Tokyo, Japan). Before SEM observation, samples should be fixed on the silicon wafer and sprayed with a metal film to enhance electrical conductivity. X-ray diffraction (XRD) of Fe-Mn-Cu@ATP powder was characterized by an advanced diffractometer Bruker D8 and carried out at 40 kV working voltage and 30 mA with K α 1 ($\lambda = 0.15405$ nm). The 2 θ scanning range was 10–80 degrees, and the scanning speed was 2 degrees per minute.

The Chemical Oxygen Demand (COD) and Biochemical Oxygen Demand (BOD₅) indexes of pharmaceutical wastewater were determined according to the standard method [29]. The ultraviolet-visible (UV-vis) light absorption spectrum of the sample was scanned by an UV-vis spectrophotometer (MAPADA/3100, Shanghai, China). The sample was placed in a 1 cm quartz cuvette, and the wavelength scanning range was 200–650 nm [30].

The change process of refractory organic compounds in pharmaceutical wastewater was analyzed by using a 3D-EEM fluorescence spectrophotometer (F7000, HACH, Loveland, CO, USA). The emission wavelength (EM) was set at 250–550 nm, and the excitation wavelength (EX) was set at 200–450 nm, and the detection scanning was performed once every 5 nm. The samples were pretreated and filtered and tested after dilution. The gas chromatography-mass spectrometer (Agilent 7890B-5977A, Santa Clara, CA, USA) was used for GC-MS analysis of organic species content and changes in samples.

3. Results and Discussion

3.1. Characterization of Catalyst

As shown in Figure 1a,c, the composite material has peaks related to Mn₂O₃ (Joint Committee on Powder Diffraction Standards: JCPDS 33-0664) at 2 $\theta = 11.3^\circ$ and 36.5 $^\circ$ and peaks related to Fe₂O₃ (JCPDS 24-0508) at 16.34 $^\circ$ and 32.9 $^\circ$, respectively. The diffraction peaks at 35.5 $^\circ$ and 61.5 $^\circ$ can be attributed to CuO phase (JCPDS 48-1548) [28,31,32]. Figure 1b shows that attapulgite modified by acid still exhibits characteristic diffraction peaks at 13.9 $^\circ$, 20.8 $^\circ$, 26.6 $^\circ$, 27.3 $^\circ$, 50.15 $^\circ$, 59.87 $^\circ$ and 68.35 $^\circ$ [33]. Compared with Figure 1c, the peak strength of metal oxide due to its load is significantly lower than that of the ATP carrier, and several distinct characteristic peaks of metal are shown. To calculate the crystal size of nanoparticles, the Debye-Scherrer formula was used (Equation (2)):

$$D = K\lambda / \beta \cos\theta, \quad (2)$$

where D is the crystal size, K is the Scherrer constant ($K = 0.89$), λ is the X-ray wavelength, β is the full width half maximum (FWHM), and θ is the diffraction angle [28,30]. Based on Equation (2), the average size of the nanocomposite is 6.91 nm. It can be seen from the SEM atlas that all of them are nanoscale. The smaller grain size may be related to the coexistence of Fe, Mn and Cu in the material. In addition, it can be seen from Figure 1 that the diffraction peaks of metal oxides and ATP overlap between 20° and 37° , and the characteristic diffraction peaks still exist, indicating that the polymetallic oxides have been successfully loaded on attapulgite.

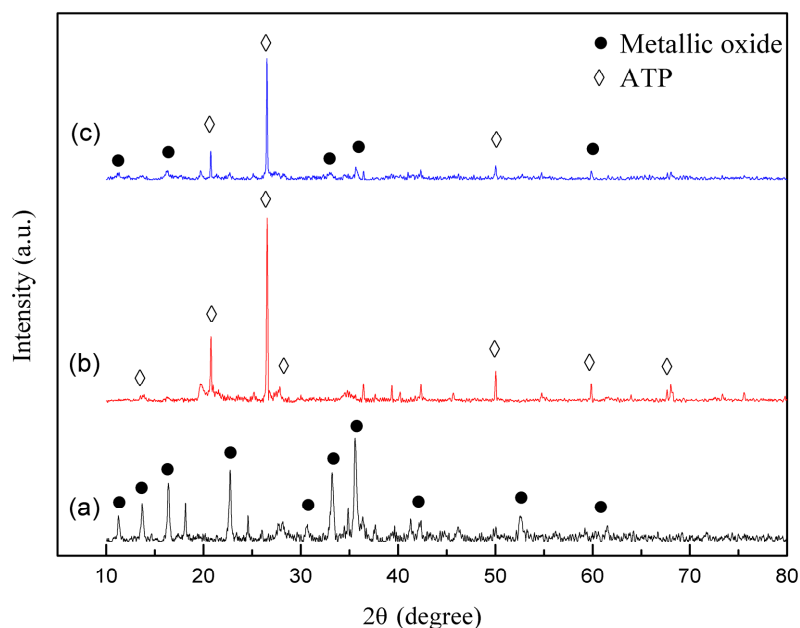


Figure 1. X-ray diffraction (XRD) patterns of (a) Fe-Mn-Cu, (b) ATP and (c) Fe-Mn-Cu@ATP.

As revealed in Figure 2, the morphologies of the original ATP, modified ATP, Fe-Mn-Cu and Fe-Mn-Cu@ATP catalysts were characterized by SEM.

Figure 2a,b showed that the surface of the original ATP soil was relatively flat and smooth, with small rod-shaped particles and agglomeration, while the surface of the modified ATP soil had a convex sand dune shape and was irregularly distributed. Its particles were larger, the structure became loose, and the colloidal impurities in the ATP pores were effectively reduced by the modification method, which can avoid the agglomeration of crystal particles to a certain extent, and help the metal particles to be loaded on the surface. In addition, relevant studies have shown that the number of internal pores and specific surface area of ATP soil soaked by hydrochloric acid will increase, and all internal impurities can also be removed [26]. The decolorization and adsorption of ATP treated with acidification will be improved, which can play a better role in the process of environmental water treatment. In Figure 2c, the nano-polymetallic oxides showed some irregular appearance, and agglomerations caused by inter-metal forces were mainly dense. In Figure 2d it can be observed that, in the Fe-Mn-Cu metal oxide, particles on the surface of ATP and dispersed evenly between the layers (compared with Figure 2b), metal oxides, and acid modified ATP together led to the roughness of the samples increased, and particles on the surface of the ATP; a large amount of deposition may be due the process of synthesis of metallic bonding. At the same time, Fe-Mn-Cu metal oxide particles generated on the ATP surface have smaller and more uniform particle size, and show better dispersion and less coaggregation. Combined with XRD results, the composite catalyst was prepared successfully.

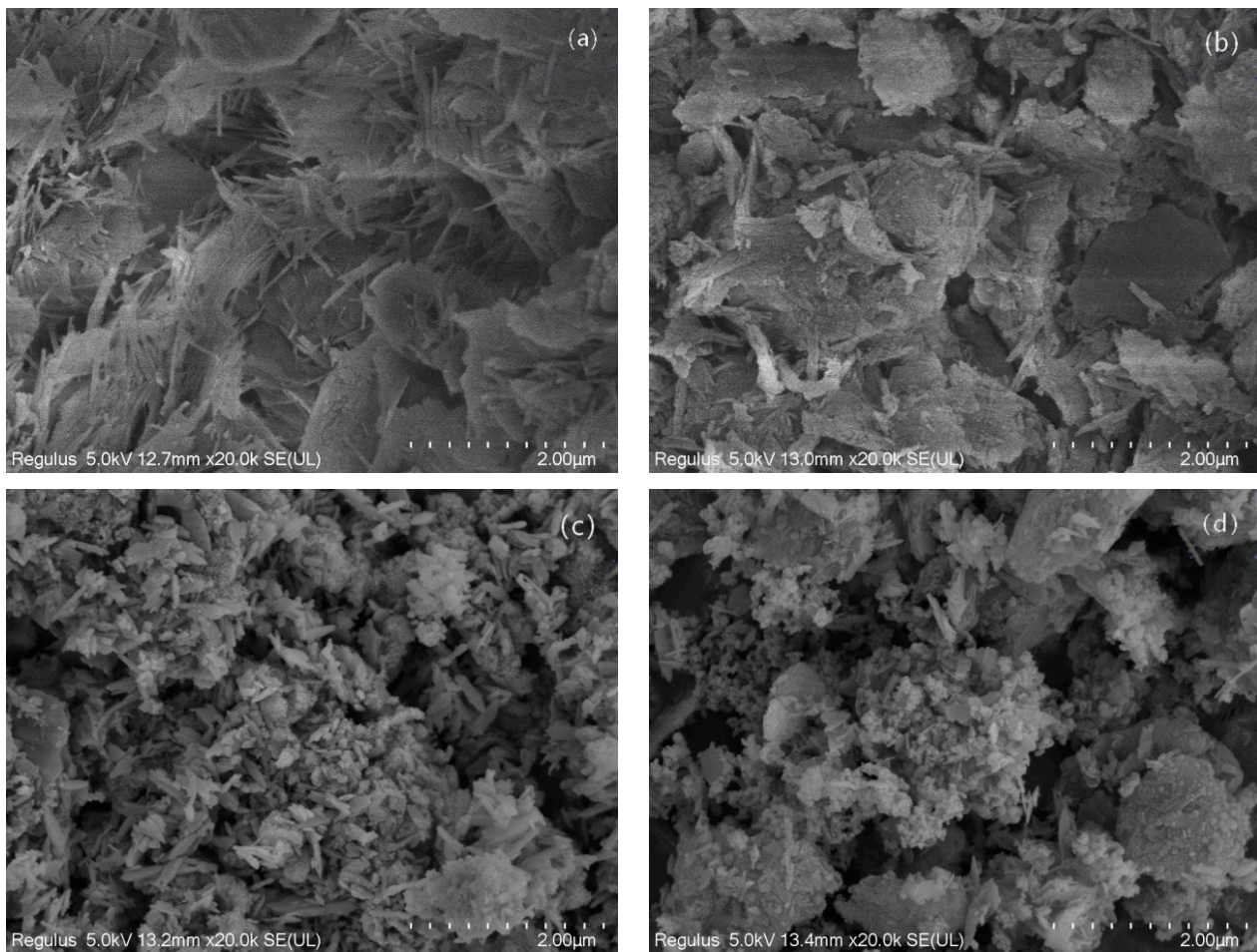


Figure 2. SEM photographs of (a) acid modified attapulgite (ATP), (b) Acid modified ATP, (c) Fe-Mn-Cu and (d) Fe-Mn-Cu@ATP.

3.2. Photo-Fenton Catalytic Degradation Performance

3.2.1. Effects of Different Treatment Systems

Different treatment methods were used to degrade the actual chemical pharmaceutical wastewater, and the COD removal rate is shown in Figure 3a. In the whole treatment process, the removal rate of COD is less than 15% after using catalyst adsorption or UV treatment alone. In addition, compared with the use of UV alone, adding oxidant can improve the COD removal by about 15%, but when adding multi-metal Fe-Mn-Cu oxide into the catalytic reaction system, the removal rate of COD can be significantly improved. Interestingly, ATP itself is not catalytic, and the removal effect of COD cannot be well improved. However, the COD removal rate of the composite catalyst catalytic system (UV/Fe-Mn-Cu@ATP/H₂O₂) was 64.9%, nearly 16% higher than that of the polymetallic catalytic system (UV/Fe-Mn-Cu/H₂O₂). The most likely reason is that nano polymetallic oxides are fixed and supported on the high surface area, which can not only prevent the accumulation of polymetallic oxides, but also prevent their loss to the water sample and improve their catalytic activity. So far, various materials have been applied to the carrier in the research process, such as graphene, activated carbon and bentonite [34,35]. Although they have a high external surface area and can help to remove COD through adsorption, their removal efficiency is still limited by the quality of wastewater and coulomb repulsive-force. Here, the acidified ATP was selected, and the surface of ATP was chemically functionalized to enhance its optimization potential and increase the formation density of •OH. ATP with high adsorption capacity and microporous structure is proved to be a low-cost carrier

for the removal of pollutants from wastewater [27]. Therefore, the composite catalyst (Fe-Mn-Cu@ATP) has been shown to perform well in photo-Fenton catalytic oxidation.

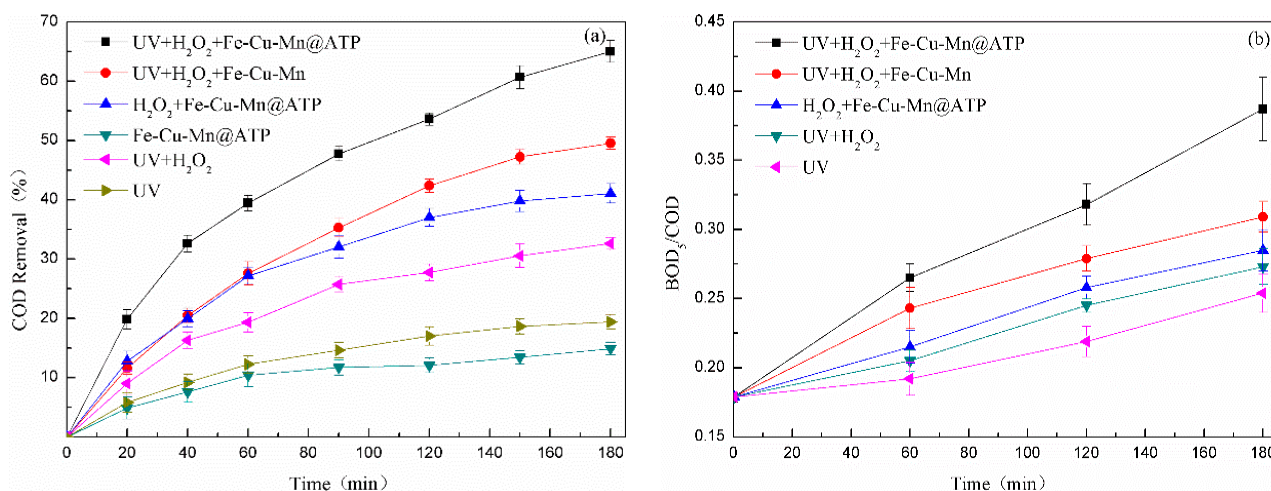


Figure 3. (a) COD removal and (b) BOD₅/COD change of the chemical pharmaceutical wastewater by different treatment systems.

According to the research results, the UV assisted Fenton can significantly improve the biodegradability of chemical pharmaceutical wastewater [36]. Figure 3b shows the treatment of BOD₅/COD by different systems in the catalytic oxidation process of UV/Fe-Mn-Cu/H₂O₂. After 180 min of treatment, BOD₅/COD in the pharmaceutical wastewater was not significantly increased by photolysis alone or catalyst adsorption, indicating that the biodegradability of the wastewater was not significantly changed by its use alone. Another key factor affecting the B/C value is H₂O₂. When its dosage as an oxidant increases from 0 to 0.5 mol/L, the B/C value also increases slightly. In contrast, UV/Fe-Mn-Cu/H₂O₂ system can significantly improve BOD₅/COD, indicating that nano polymetallic oxides have certain catalytic activity and play a certain catalytic role in the photocatalytic oxidation process, but the highest BOD₅/COD is 0.309, and the biodegradability of effluent is not high. After replacing the catalyst with the prepared Fe-Mn-Cu@ATP, the effluent BOD₅/COD reached 0.387, proving that Fe-Mn-Cu@ATP has stronger catalytic activity than the single polymetallic oxide, which may be related to the reduction of particle aggregation due to the loading of polymetallic materials with large specific surface area. It has been proved that ATP has high adsorption capacity, can decolorize and adsorb pollutants in wastewater, and has low cost. Moreover, the composite nano Fe-Mn-Cu@ATP is more exposed to •OH than the polymetallic oxide Fe-Mn-Cu, so it can be proved that the composite catalyst performs better in photo-Fenton catalysis.

3.2.2. Effect of the Initial pH

Initial pH of solution is the main operating parameter that affects the efficiency of the system. In order to more reliably analyze the effect of initial pH for processing, according to the previous experimental data, the influence of initial pH on pharmaceutical wastewater was analyzed under the conditions of peroxide concentration of 0.5 mol/L, catalyst dosage of 10 g/L and optical distance of 10 cm.

Figure 4 showed the effect of initial pH on COD removal rate and the change of BOD₅/COD in pharmaceutical wastewater. It can be seen from Figure 4a that when pH increased from 1.0 to 10.0, the COD removal rate first increased and then decreased, indicating that the catalyst activity has a significant dependence on pH. At the initial pH of 2.0, the COD removal rate was optimal. Initial pH solution for lower or higher are unfavorable to COD removal. The reason may be that the hydroxyl free radical (•OH) oxidation reduction potential is higher; under the low pH value, its formation rate increased, but when

the pH is too low, an excess of H^+ in the solution can react with hydroxyl radicals, thus affecting the reaction system of organic pollutants treatment effect. When pH continues to rise to neutral or even alkaline, H_2O_2 will be decomposed into O_2 , and H_2O_2 will be inhibited to decompose into hydroxyl radicals, thus reducing the production of hydroxyl radicals. On the other hand, under alkaline conditions, the negative charge on the surface of the catalyst is not conducive to the adsorption of pollutants to its surface, thus reducing the catalytic effect. In the hydroxyl radical oxidation pharmaceutical wastewater system, under the condition of low pH, chlorine ion accelerated the degradation process, while under the condition of high pH, chlorine ion significantly inhibited the degradation process. This phenomenon is consistent with the results of this study. According to the results, the UV/Fe-Mn-Cu@ATP/ H_2O_2 system can specifically adsorb and degrade organic pollutants. Compared with the single photocatalysis or Fenton-like system, it is more effective and more suitable for chemical pharmaceutical wastewater. According to Figure 4a, pH of 2.0 leads to a slightly higher BOD_5/COD value. This result can be interpreted that, under the condition of pH = 2.0, there are more hydroxyl radicals produced, which can attack organic compounds in chemical pharmaceutical wastewater and lead to further mineralization, and the reaction conditions are the most favorable [37]. This is consistent with the above analysis.

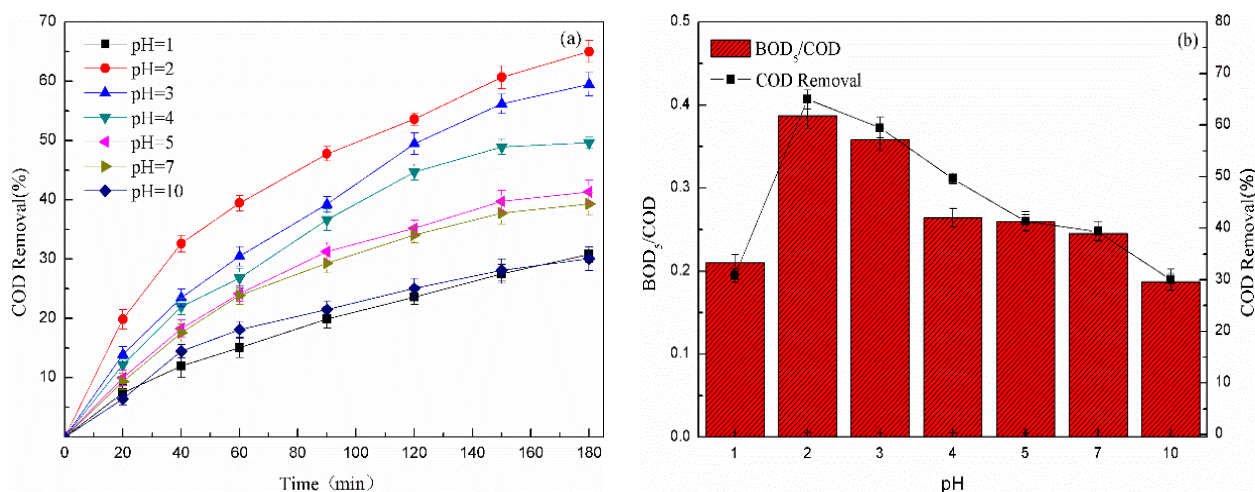


Figure 4. Effect of initial pH on (a) COD removal and (b) BOD_5/COD of chemical pharmaceutical wastewater (Fe-Mn-Cu@ATP dose = 10.0 g/L, hydrogen peroxide concentration = 0.5 mol/L, light distance = 20 cm).

3.2.3. Effect of the Catalyst Dosage

After initial pH was determined to be 2.0 and other conditions remained unchanged, the dosage of catalyst was changed from 2.0 g/L to 12.0 g/L to investigate the treatment effect of catalytic oxidation pharmaceutical wastewater.

Figure 5 showed the effect of catalyst dosage on COD removal and BOD_5/COD value. The results showed that the COD removal rate increased from 33.7% to 53.3% when the catalyst dosage increased from 2.0 g/L to 12.0 g/L. When hydrogen peroxide is an oxidant, the higher the dosage of the catalyst, the more metal active sites can be provided for H_2O_2 . However, when the Fe-Mn-Cu@ATP dosage is increased from 2.0 g/L to 10.0 g/L, the COD removal rate reached the highest. Some studies have shown that when the catalyst content in the reaction system is low, there are fewer active sites in the system, which are not enough to promote the rapid decomposition of H_2O_2 to produce hydroxyl radicals, thereby affecting the degradation effect [38]. However, no significant advantage in COD removal was observed when too much catalyst was used. The high catalyst dosage will limit the further acceleration of the reaction rate, and easily lead to the generation of electron-hole effect to generate superoxide radicals with weaker oxidation capacity than that of $\bullet OH$, which will reduce the catalytic performance of the

reaction system. In addition, this phenomenon can also be attributed to the reaction between excess Fe(II), Cu(I), Mn(II) active sites and $\bullet\text{OH}$ on the surface of Fe-Mn-Cu@ATP (Equations (3)–(5)). Excess catalyst may consume part of $\bullet\text{OH}$, which acts as a hydroxyl radical scavenger [39].

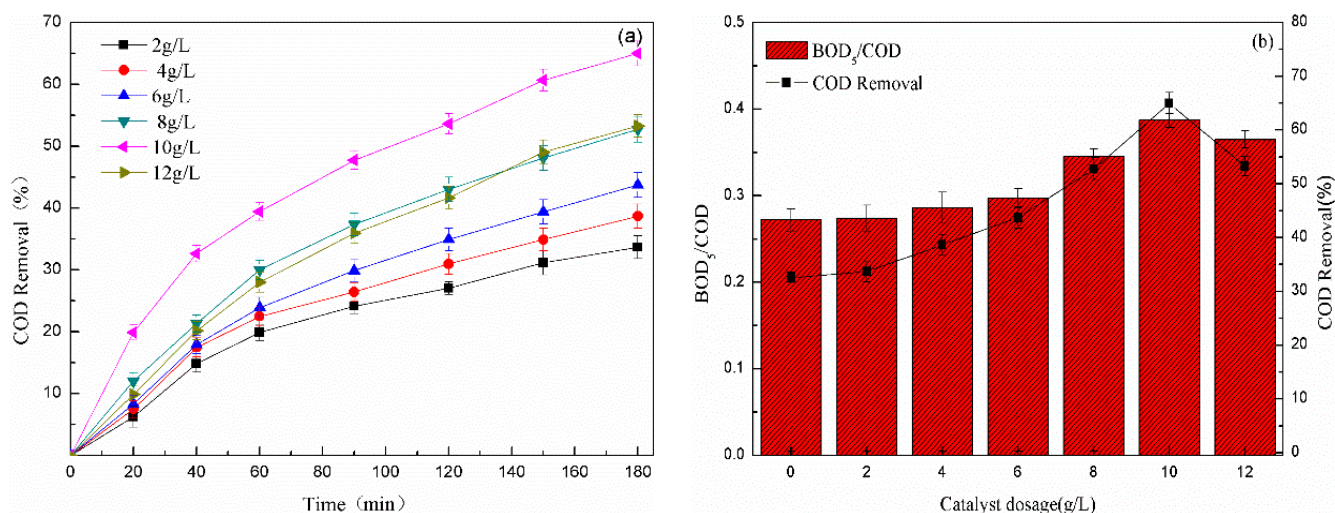
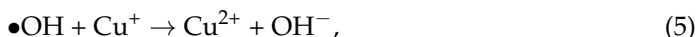
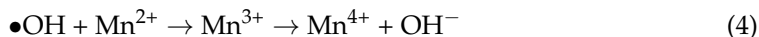
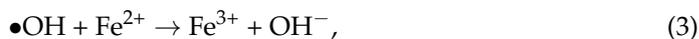


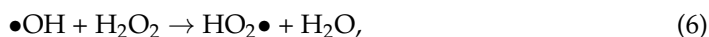
Figure 5. Effect of catalyst dosage on (a) COD removal and (b) BOD₅/COD of pharmaceutical wastewater (initial pH = 2.0, hydrogen peroxide concentration = 0.5 mol/L, light distance = 20 cm).

In addition, the effect of catalyst dosage on biodegradability is shown in Figure 5b. In the photo-assisted Fenton-like catalytic oxidation process, increasing the amount of catalyst has a good effect on improving BOD₅/COD. The results showed that the biodegradability of all samples was increased to varying degrees after being treated for 180 min. The BOD₅/COD without catalyst was 0.273, while that of 10.0 g/L nano-Fe-Mn-Cu@ATP was 0.387. This may be related to the more active sites of UV and hydroxyl radical interaction with the increase of catalyst and dosage, which led to the significant enhancement of biodegradability of pharmaceutical wastewater. Therefore, 10.0 g/L was chosen as the catalyst usage in the experiment.

3.2.4. Effect of the Peroxide Concentration

In order to reveal the influence of hydrogen peroxide concentration, at room temperature, other conditions were kept constant, and the catalytic degradation effect of the amount of oxidant H₂O₂ on pharmaceutical wastewater was investigated.

Figure 6a showed the degradation effect of Fe-Mn-Cu@ATP system on wastewater under different oxidant dosages. The COD removal rate increased from 33.09% at 0.1 mol/L to 64.98% at 0.5 mol/L. It can be seen that with the increase of oxidant concentration, the COD removal rate will directly improve [40]. In the experiment, within a certain range, as the dosage of H₂O₂ increases, it will promote the production of more $\bullet\text{OH}$. However, excessive use of H₂O₂ may lead to the quenching of hydroxyl radical, thus reducing the catalytic effect [41,42]. This phenomenon can be expressed as the following reaction (Equations (6) and (7)).



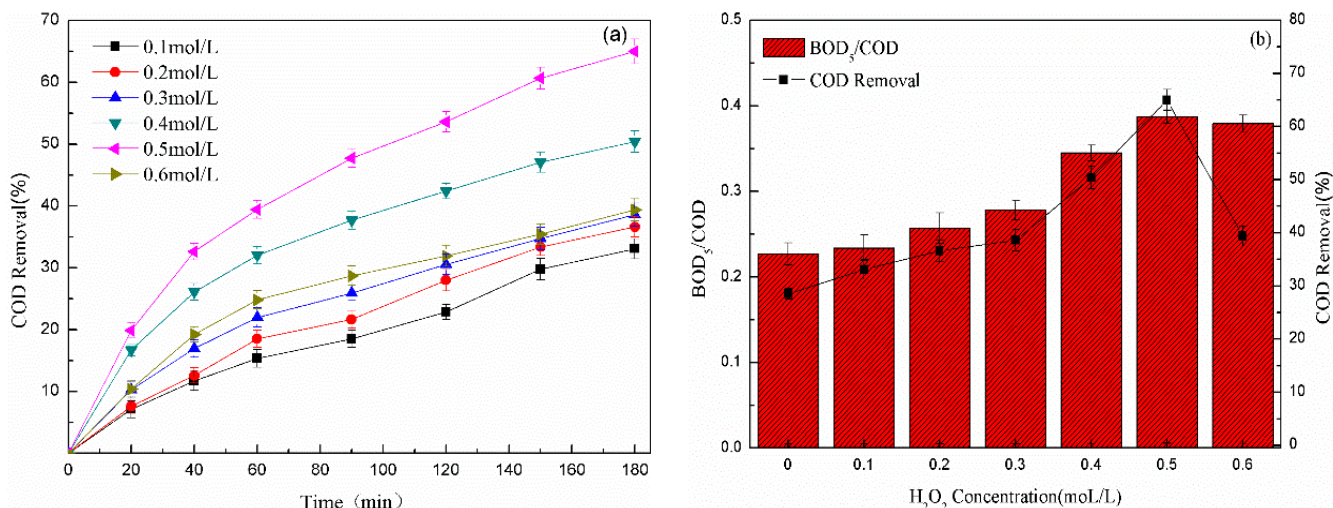


Figure 6. Effect of H₂O₂ concentration on (a) COD removal and (b) BOD₅/COD of pharmaceutical wastewater (initial pH = 2.0, catalyst dosage = 10.0 mol/L, light distance = 20 cm).

As shown in Figure 6b, the higher the oxidant concentration, the higher the BOD₅/COD value. When H₂O₂ concentration increased from 0.1 mol/L to 0.5 mol/L, the value of BOD₅/COD increased from 0.23 to 0.387. In the process of photo-assisted Fenton-like treatment, the gradual degradation of organic base system made the B/C value increase gradually, including the degradation of organic compounds that can improve the biodegradability, degradation or reduction of toxic substances in wastewater, and oxidation of organic matter into carbon dioxide, water and inorganic compounds. Therefore, in the heterogeneous system, the higher oxide concentration can improve BOD₅/COD, but the further increase of the amount of H₂O₂ did not significantly improve the removal rate of COD and BOD₅/COD. Therefore, 0.5 mol/L H₂O₂ was selected for further study.

3.2.5. Effect of UV Light Distance

The chemical pharmaceutical wastewater with initial pH of 2.0 was placed in the reactor, the catalyst dosage was 10 g/L, the H₂O₂ concentration was 0.5 mol/L, the illumination distance was changed, and the blank sample was controlled to investigate the effect of light intensity on COD removal rate and BOD₅/COD. The experimental results are shown in the Figure 7.

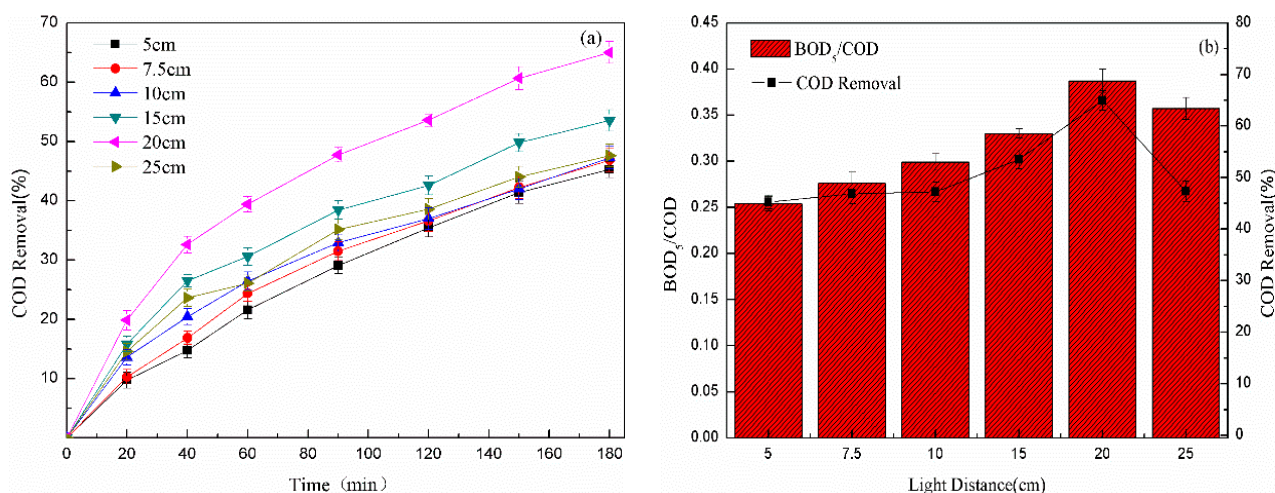


Figure 7. Effect of light distance on (a) COD removal and (b) BOD₅/COD of pharmaceutical wastewater (initial pH = 2.0, hydrogen peroxide dosage = 0.5 mol/L, light distance = 20 cm).

It can be seen from Figure 7 that the change of light distance makes no obvious change in the removal of COD and the improvement of biodegradability. On the whole, as the illumination distance decreases gradually, the catalytic effect (including COD removal and BOD₅/COD) first increases and then decreases. The smaller the optical distance, the greater the light intensity, and the more photons that hit the surface of the catalyst, the more electron-hole pairs can be excited. With the further reduction of the light distance and the increase of light intensity, COD removal and BOD₅/COD both decrease instead of increasing [43]. This may be due to two reasons: one is the inhibition of chlorine ions. There are a large number of chlorine ions in wastewater, which compete $\bullet\text{OH}$ with organics matter. Studies have shown that the reaction rate of chlorine ion with $\bullet\text{OH}$ ($k_{\bullet\text{OH}\cdot\text{Cl}^-} = 4.3 \times 10^9 \text{ L}\cdot(\text{mol}\cdot\text{s})^{-1}$), which is higher than that of some organic compounds with $\bullet\text{OH}$, thus inhibiting the degradation reaction of chemical pharmaceutical wastewater [34]. On the other hand, there is an addition reaction. When the light intensity is too high, the chlorine ions in the wastewater will compete for oxygen with the organic matter and generate hypochlorous acid. Under the strong light radiation, chlorine free radical will be generated, and then the addition reaction will occur with the organic matter to increase the COD. Secondly, when the light distance is too small, the ultraviolet lamp will heat the solution for a long time, which will cause secondary pollution. Therefore, the illumination distance of 20 cm was chosen as the best in this experiment.

3.3. Variations of Organic Compounds

3.3.1. 3D-EEM the Fluorescence Spectrum Analysis

In order to better understand the changes of organic matter in the wastewater treated by UV/Fe-Mn-Cu@ATP/H₂O₂, the chemical changes of organic matter in pharmaceutical wastewater were determined by using 3D electron microscope (3D-EEM) spectroscopy.

According to the literature research [44], the fluorescence spectrum can be divided into five major areas, which represent aromatic protein substances I(I), aromatic protein substances II(II), fulvic acid (FA) chemicals (III), soluble microbial metabolites (IV) and humic acid (HA) substances (V). It can be seen from Figure 8a that, before the reaction, there is obviously a major EEM peak in pharmaceutical wastewater: The peak A, at EX/EM of 450/525 nm, was labeled as HA substances. At this time, the complex component of FA and HA in wastewater was the largest. This indicated that the water sample was in a difficult state before pretreatment.

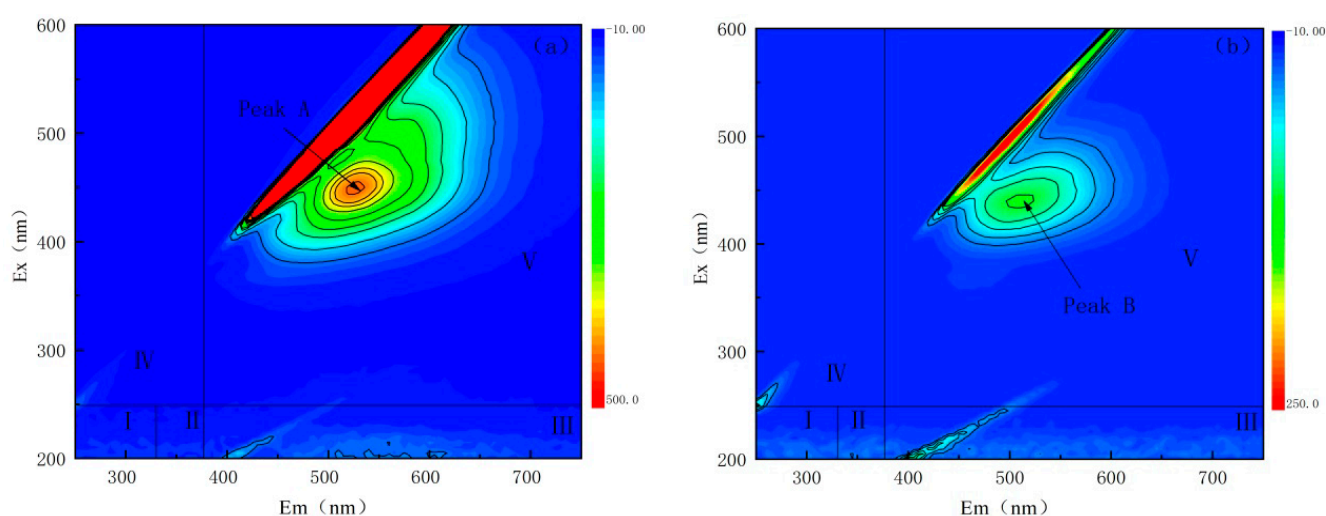


Figure 8. 3D-excitation emission matrix fluorescence spectroscopy of (a) input pharmaceutical wastewater and (b) treated pharmaceutical wastewater.

As can be seen from Figure 8b, the maximum fluorescence intensity EX/EM of the new peak (B) was 440/505 nm after the catalytic treatment for 180 min, which may be

derived from visible HA compounds. This may be caused by the accumulation of non-degradable humus. After catalytic reaction with Fe-Mn-Cu@ATP, the peak A shifted and the fluorescence intensity was significantly reduced, indicating that some FA and HA were effectively degraded into substances without fluorescence characteristics, which was consistent with the analysis results of GC-MS, indicating that FA and HA were effectively degraded into small molecules or removed, thereby improving the biodegradability of the effluent [40].

3.3.2. GC-MS Organic Compounds Change Analysis

Gas chromatography-mass spectrometry (GC-MS) was used to detect the raw water and treated effluent of chemical pharmaceutical wastewater. The analysis of the change of organic matter is shown in Table 2.

Table 2. Organic matter changes in pharmaceutical wastewater before and after the reaction.

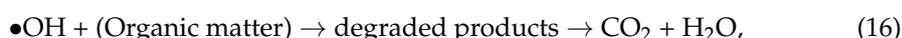
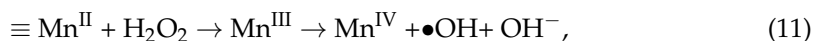
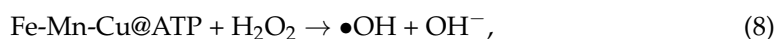
Organic Compounds	Initial Values		Final Values	
	Peak Area	P (%)	Peak Area	P (%)
Pyrimidine, 2-chloro	134,337,798	18.86	112,957,014	31.23
2,6-Dichloropyrazine	311,329,997	43.72	2,072,863	0.57
Pyrimidine, 4,6-dichloro	109,383,005	15.36	86,220,168	23.84
Diethyl carbitol	532,383	0.07	N.D.	N.D.
4-Amino-2,6-dichloropyridine	180,401	0.03	N.D.	N.D.
2,4-Dihydroxybenzaldehyde, 2TMS derivative	358,603	0.05	472,319	0.13
Cyclo-penta-siloxane, deca-methyl	3,375,447	0.47	2,703,467	0.75
Pyrimidine, 2,4,6-trichloro	145,047,498	20.37	21,144,132	5.85
Benzoic acid, 2,6-dichloro-, 2-acetylphenyl ester	158,224	0.02	N.D.	N.D.
Benzene,1-chloro-3,5-difluoro-	228,041	0.03	N.D.	N.D.
Pyrimidine, tetrachloro	371,995	0.05	N.D.	N.D.
4-Chloroquinoline	300,677	0.04	N.D.	N.D.
Cyclo-hexa-siloxane, dodeca-methyl	4,558,815	0.64	3,698,006	1.02
2-Bromo-1,3-thiazole-5-carbaldehyde	618,021	0.09	N.D.	N.D.
Benzenamine, 2,3,4-trichloro	166,015	0.02	N.D.	N.D.
Cyclo-hepta-siloxane, tetra-deca-methyl	800,715	0.11	1,155,308	0.32
2,4-Dichloroquinoline	422,801	0.06	N.D.	N.D.
1,3-Dioxolane	N.D.	N.D.	240,275	0.07
4-Methyl-2,4-bis(p-hydroxyphenyl) pent-1-ene, 2TMS derivative	N.D.	N.D.	10,638,907	2.94
Imidazo[1,5-a]pyridine, 3-phenyl	N.D.	N.D.	357,153	0.10
Pyrimidine, 4-chloro-2-methyl	N.D.	N.D.	119,229	0.03
N-(2,6-Diethylphenyl)-1,1,1-trifluoro-methane sulfonamide	N.D.	N.D.	117,811,503	32.58
Cyclotrisiloxane, hexamethyl	N.D.	N.D.	998,827	0.28
Naphthalene, 2-chloro	N.D.	N.D.	338,243	0.09
2H-imidazole-2-thione, 1,3-dihydro-4-(2-methylpropyl)	N.D.	N.D.	177,569	0.05
1-Nonadecanol, TMS derivative	N.D.	N.D.	236,706	0.07
Ethyne, 1-bromo-2-trimethylsilyl	N.D.	N.D.	99,410	0.03
3,4-Dihydroxyphenylglycol, 4TMS derivative	N.D.	N.D.	156,565	0.04
2,5,8-Triphenyl benzo-triazazole	N.D.	N.D.	63,392	0.02

P (%): mass percentage, was calculated according to the peak area. N.D.: not detected.

After optimizing the catalytic conditions, the species and mass percentage of organic compounds obtained by UV/Fe-Mn-Cu@ATP/H₂O₂ treatment were significantly changed compared with raw water. The peak areas of 2,4-Dihydroxybenzaldehyde and Cyclo-hexa-siloxane, dodeca-methyl increased slightly after treatment, while the peak areas of other types of structurally complex organic substances all decreased significantly. In the original pharmaceutical wastewater, 17 organic pollutants were detected, among which nine organic pollutants were completely removed in the catalytic reaction. This was especially true for heterocyclic compounds, esters, and ethers, such as 4-Amino-2,6-dichloropyridine, Pyrimidine, tetrachloro, Diethyl carbitol, Benzoic acid, 2,6-dichloro-,

2-acetylphenyl ester, etc., have been well removed. Among them, the removal effect of heterocyclic compounds was the most obvious. The results showed that the Fenton-like method with the participation of a catalyst could degrade nitrogen-containing heterocyclic organic compounds into degradable substances. The most likely reason for this result is that heterocyclic compounds and long-chain hydrocarbons were destroyed by $\bullet\text{OH}$, which formed some intermediate products or eventually become carbon dioxide and water. The addition of intermediate products such as alkanes (derivatives) and alkynes in the effluent indicated that organic pollutants in the original wastewater were attacked by $\bullet\text{OH}$, promoting their transformation into simpler substances. The literature mentions that H_2O_2 reacts with metal oxides composite catalyst to accelerate the formation of $\bullet\text{OH}$, which also proved the ability of the multi-metal composite catalyst to quickly catalyze hydrogen peroxide to produce $\bullet\text{OH}$, accelerate the oxidation process of the system, and further mineralize pharmaceuticals wastewater [19]. Similar results were obtained in earlier studies [45,46].

There are probably three main reaction mechanisms in the Fe-Mn-Cu@ATP catalyzed photo-Fenton treatment system: ultraviolet reaction with hydrogen peroxide, direct reaction between catalyst and hydrogen peroxide, and indirect reaction between free radicals generated by interaction between UV and hydrogen peroxide and catalyst reaction. All these three reactions can take place on the surface of the catalyst and in the solution, while Fe-Mn-Cu@ATP has a certain adsorption effect. On its surface, it can react with H_2O_2 and organic matter, the consumed metal ions can be effectively regenerated under UV light, and $\bullet\text{OH}$ can be converted into intermediate products catalytically, finally generating small molecules of organic matter with simple structure, which is convenient for subsequent further treatment [47,48]. These envisaged mechanisms could be simplified as follows (Equations (8)–(16)):



3.3.3. UV-Vis Absorption Spectrum Analysis

Figure 9 shows the change process of ultraviolet-visible (UV-vis) spectrum with photo-Fenton catalytic oxidation time. It can be observed that the shape and trend of UV-vis pattern at different processing times are similar, and the overall absorption intensity increases gradually with the decrease of wavelength. The initial spectrum has a very distinct shoulder around the wavelength of 270 nm. During the treatment, as the reaction time goes by, a significant decrease in absorbance can be observed, which was due to the oxidative degradation of the chromogenic part of the soluble organic compounds. This result is consistent with Ma's previous research [30]. During the reaction process, $\bullet\text{OH}$ has a tendency to preferentially attack the organic part that was absorbed in the 260–280 nm wavelength range. After 180 min of UV/Fe-Mn-Cu@ATP/ H_2O_2 catalytic oxidation reaction, the shoulder almost disappeared completely.

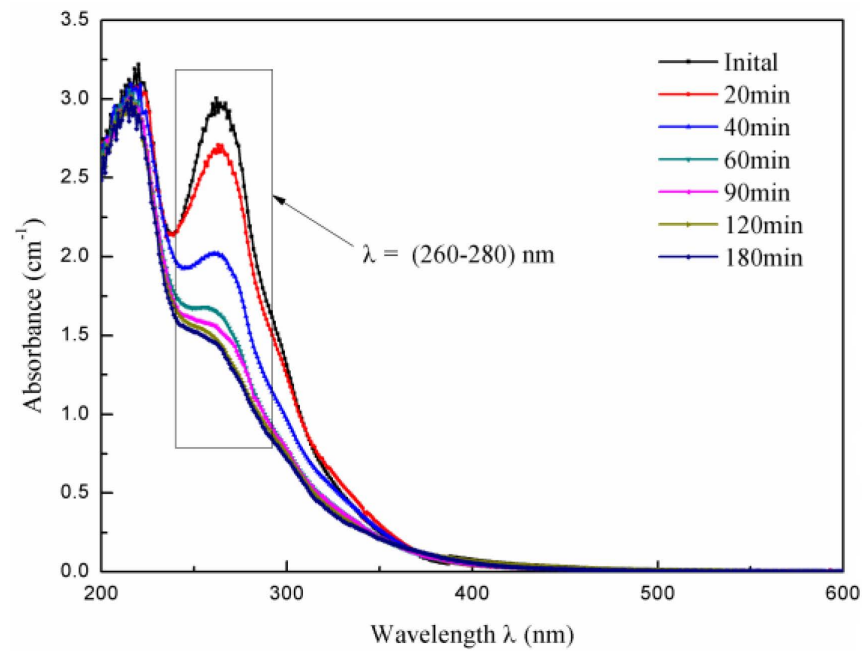


Figure 9. Evolution of UV-vis spectrum in catalytic oxidation of chemical pharmaceutical wastewater.

3.4. Degradation Mechanism of Photo-Fenton Catalytic Oxidation

In order to study the mechanism of the Fe-Mn-Cu@ATP catalyzed photo-Fenton reaction system, a free radical quenching experiment was carried out. According to the literature reports, hydroxyl radicals ($\bullet\text{OH}$) are the main active factors that play a role in the photo-Fenton system, and superoxide radicals ($\bullet\text{O}_2^-$) and holes (h^+) are also common. Therefore, this experiment designed a capture experiment for hydroxyl radicals. During the reaction, tertiary butyl alcohol ($\text{C}_4\text{H}_{10}\text{O}$, capture of $\bullet\text{OH}$), KI (capture of h^+ and $\bullet\text{OH}$), para-benquinone (BQ, capture of $\bullet\text{O}_2^-$) and ethylenediamine tetra-acetic acid disodium sodium (EDTA-2Na, capture of h^+) were used as capture agents to detect free radicals in the reaction process. The results are shown in the Figure 10.

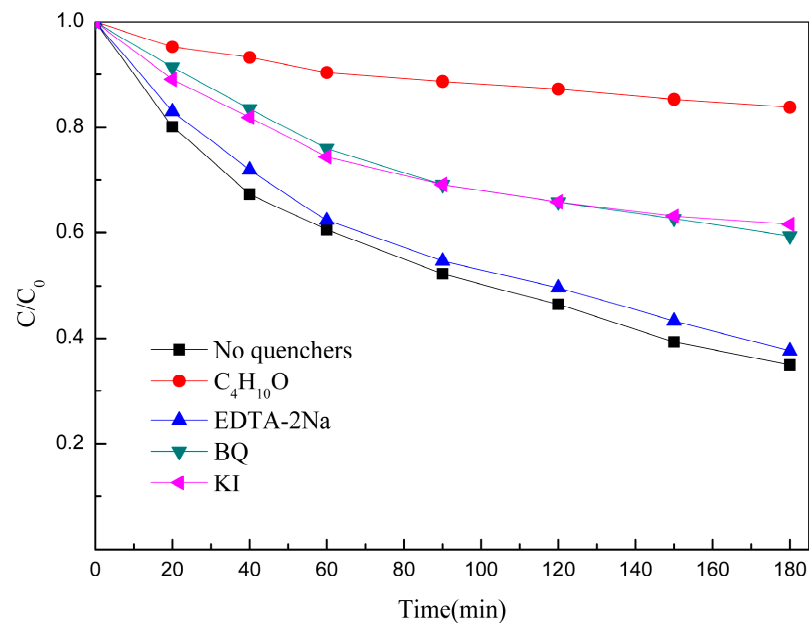


Figure 10. Effects of different group capture factors on COD removal of pharmaceutical wastewater.

After 180 min of photo-Fenton catalysis, it was found that the addition of EDTA-2Na had no significant effect on the degradation effect of COD compared with the treatment effect without capture agent, indicating that h^+ only accounted for a very small part of the reaction process and was not the main active factor, which was also confirmed from the change curve results of adding BQ and KI. The addition of $C_4H_{10}O$ and BQ capture agents both reduced the treatment efficiency and inhibited the oxidative activity of their respective groups to varying degrees, and the inhibitory effect was $C_4H_{10}O > KI > BQ$. In summary, when the Fe-Mn-Cu@ATP catalyzed photo-Fenton reaction system degraded pharmaceutical wastewater, $\bullet OH$ played the most important role in the system, and is the main active free radical in the process of single bond oxidation and catalytic oxidation [49].

3.5. The Stability of the Catalyst

The stability of the recoverable catalyst is an important index to evaluate its performance. Therefore, the repeatability test was carried out after the recovery and retreatment of the catalyst in pharmaceutical wastewater. The catalyst was recovered through filtration and calcination. As shown in Figure 11, after six cycles of recycling, the catalyst still maintained its original catalytic activity and the COD removal was 59%. Compared with the first treatment, slight loss was observed, indicating that the prepared catalyst was of good stability. Different from the traditional binary ferrite, the catalyst has higher catalytic activity and cycling stability [50]. This work could provide a new research idea for the design of a photo-Fenton catalyst.

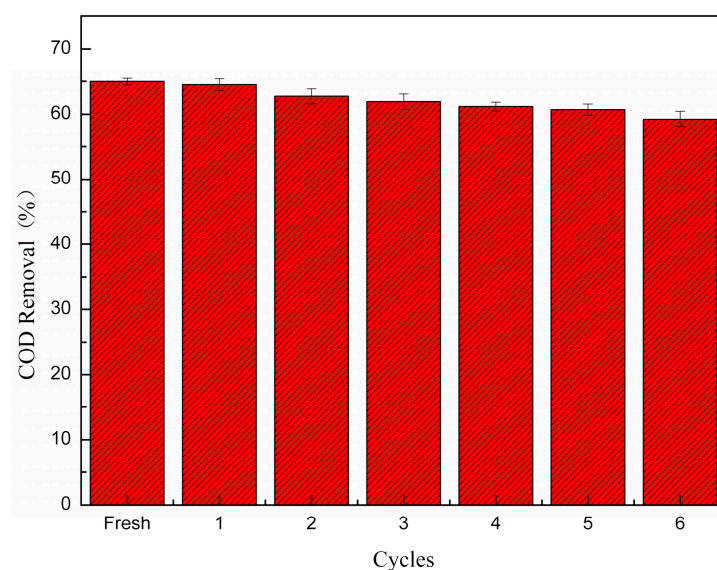


Figure 11. Effect of recycling the catalyst on COD removal (initial pH of 2.0; Catalyst dosage of 10.0 g/L; The concentration of H_2O_2 is 0.5 mol/L; The illumination distance is 20 cm).

4. Conclusions

Photo-Fenton combined with nano Fe-Mn-Cu@ATP catalyst (UV/Fe-Mn-Cu@ATP/ H_2O_2) has been proved to be an effective advanced oxidation degradation technology for pretreatment of refractory pollutants in pharmaceutical wastewater. When the catalyst dosage was 10 g/L, the hydrogen peroxide dosage was 0.5 mol/L and the pH was 2.0, the COD removal reached 64.9%, and the BOD_5/COD increased from 0.179 to 0.387 after 180 min of reaction time. The results of GC-MS and 3D-EEM showed that refractory compounds, such as humic and fulvic acid (HA and FA), were degraded to low molecular weight intermediates by photo-Fenton, and the biodegradability of wastewater has been improved through a low-cost degradation system, which could be further promoted by a biological process. Finally, it was speculated that the nano Fe-Mn-Cu/ATP catalyst treated the formation

of •OH and clarified the main mechanism of the degradation of refractory pollutants by photo-Fenton combined with a nano Fe-Mn-Cu-ATP@ATP catalyst.

Author Contributions: Conceptualization, M.L. and Z.H.; methodology, M.L.; software, M.L.; validation, M.L., J.W. and Y.W.; formal analysis, M.L.; investigation, M.L.; resources, Z.H.; data curation, M.L.; writing—original draft preparation, M.L.; writing—review and editing, Z.H.; visualization, M.L.; supervision, Z.H.; project administration, Z.H.; funding acquisition, Z.H. All authors have read and agreed to the published version of the manuscript.

Funding: This work was financially supported by China's National Key Project of Science and Technology (No. 2017ZX07602-001-002).

Informed Consent Statement: Not applicable.

Data Availability Statement: Data available on request due to the restriction of privacy. The data presented in this study are available on request from the corresponding author. The data are not publicly available due to we also need to use these data for further research, involving privacy.

Conflicts of Interest: The authors declare no conflict of interest. The funders had no role in the design of the study; in the collection, analyses, or interpretation of data; in the writing of the manuscript; nor in the decision to publish the results.

References

1. Anliker, S.; Patrick, M.; Fenner, K.; Singer, H. Quantification of Active Ingredient Losses from Formulating Pharmaceutical Industries and Contribution to Wastewater Treatment Plant Emissions. *Environ. Sci. Technol.* **2020**, *54*, 15046–15056. [[CrossRef](#)] [[PubMed](#)]
2. Chen, H.L.; Zhang, X.T.; Wang, Q.; Yao, P.L. Metagenomic Analysis of Antibiotic Resistant Bacteria and Resistance Genes in a Pharmaceutical and Chemical Wastewater Treatment Plant. *Huan Jing Ke Xue* **2020**, *41*, 313–320.
3. Gadipelly, C.; Pérez-González, A.; Yadav, G.D.; Ortiz, I.; Ibáñez, R.; Rathod, V.K.; Marathe, K.V. Pharmaceutical Industry Wastewater: Review of the Technologies for Water Treatment and Reuse. *Ind. Eng. Chem. Res.* **2014**, *53*, 11571–11592. [[CrossRef](#)]
4. Behfar, R.D.R.; Heydari, R. Pharmaceutical Wastewater Chemical Oxygen Demand Reduction: Electro-Fenton, UV-enhanced Electro-Fenton and Activated Sludge. *Int. J. Eng.* **2019**, *32*, 1710–1715.
5. Jhunjhunwala, A.; Pathak, U.; Sarkar, K.K.; Majee, S.; Mandal, D.D.; Mandal, T. Removal of levosulpiride from pharmaceutical wastewater using an advanced integrated treatment strategy comprising physical, chemical, and biological treatment. *Environ. Prog. Sustain. Energy* **2020**. [[CrossRef](#)]
6. Kirchon, A.; Zhang, P.; Li, J.; Joseph, E.A.; Chen, W.; Zhou, H.C. Effect of Isomorphic Metal Substitution on the Fenton and Photo-Fenton Degradation of Methylene Blue Using Fe-Based Metal-Organic Frameworks. *ACS Appl. Mater. Interfaces* **2020**, *12*, 9292–9299. [[CrossRef](#)] [[PubMed](#)]
7. Zhang, Y.; Liu, C.; Xu, B.; Qi, F.; Chu, W. Degradation of benzotriazole by a novel Fenton-like reaction with mesoporous Cu/MnO₂: Combination of adsorption and catalysis oxidation. *Appl. Catal. B Environ.* **2016**, *199*, 447–457. [[CrossRef](#)]
8. Chong, S.; Zhang, G.; Zhang, N.; Liu, Y.; Huang, T.; Chang, H. Diclofenac degradation in water by FeCeO_x catalyzed H₂O₂: Influencing factors, mechanism and pathways. *J. Hazard. Mater.* **2017**, *334*, 150–159. [[CrossRef](#)]
9. Cen, H.; Nan, Z. Monodisperse Zn-doped Fe₃O₄ formation and photo-Fenton activity for degradation of rhodamine B in water. *J. Phys. Chem. Solids* **2018**, *121*, 1–7. [[CrossRef](#)]
10. Ran, G.; Li, Q. Degradation of refractory organic compounds from dinitro-diazophenol containing industrial wastewater through UV/H(2)O(2) and UV/PS processes. *Environ. Sci. Pollut. Res. Int.* **2020**, *27*, 6042–6051. [[CrossRef](#)]
11. Xu, Z.; Zheng, R.; Chen, Y.; Zhu, J.; Bian, Z. Ordered mesoporous Fe/TiO₂ with light enhanced photo-Fenton activity. *Chin. J. Catal.* **2019**, *40*, 631–637. [[CrossRef](#)]
12. Wu, Z.; Wang, X.; Zhang, X.; Zhang, Y.; Wang, Y.; Sun, S.; Wu, W. Nanostructured Semiconductor Supported Iron Catalysts for Heterogeneous Photo-Fenton Oxidation: A Review. *J. Mater. Chem. A* **2020**, *8*, 15513–15546.
13. Gogoi, A.; Navgire, M.; Sarma, K.C.; Gogoi, P. Fe₃O₄-CeO₂ metal oxide nanocomposite as a Fenton-like heterogeneous catalyst for degradation of catechol. *Chem. Eng. J.* **2017**, *311*, 153–162. [[CrossRef](#)]
14. Ahmad, I. Comparative study of metal (Al, Mg, Ni, Cu and Ag) doped ZnO/g-C₃N₄ composites: Efficient photocatalysts for the degradation of organic pollutants. *Sep. Purif. Technol.* **2020**, *251*, 117372. [[CrossRef](#)]
15. Nichela, D.A.; Berkovic, A.M.; Costante, M.R.; Juliarena, M.P.; García Einschlag, F.S. Nitrobenzene degradation in Fenton-like systems using Cu(II) as catalyst. Comparison between Cu(II)- and Fe(III)-based systems. *Chem. Eng. J.* **2013**, *228*, 1148–1157. [[CrossRef](#)]
16. Zhang, X.; Ding, Y.; Tang, H.; Han, X.; Zhu, L.; Wang, N. Degradation of bisphenol A by hydrogen peroxide activated with CuFeO₂ microparticles as a heterogeneous Fenton-like catalyst: Efficiency, stability and mechanism. *Chem. Eng. J.* **2014**, *236*, 251–262. [[CrossRef](#)]

17. Li, K.; Zhao, Y.; Song, C.; Guo, X. Magnetic ordered mesoporous Fe₃O₄/CeO₂ composites with synergy of adsorption and Fenton catalysis. *Appl. Surf. Sci.* **2017**, *425*, 526–534. [[CrossRef](#)]
18. Jauhar, S.; Singhal, S.; Dhiman, M. Manganese substituted cobalt ferrites as efficient catalysts for H₂O₂ assisted degradation of cationic and anionic dyes: Their synthesis and characterization. *Appl. Catal. A Gen.* **2014**, *486*, 210–218. [[CrossRef](#)]
19. Su, Y.; Li, M.; Ge, M. Catalytic Degradation of Poly(Vinyl Alcohol) by Fe_xMn_yCu_zO_w/γ-Al₂O₃ Nano-particles Catalyst Using Box-Behnken Design. *Fibers Polym.* **2019**, *20*, 1774–1783. [[CrossRef](#)]
20. Litter, M.I.; Slodowicz, M. An overview on heterogeneous Fenton and photoFenton reactions using zerovalent iron materials. *J. Adv. Oxid. Technol.* **2017**, *20*, 160–164. [[CrossRef](#)]
21. Singh, L.; Rekha, P.; Chand, S. Cu-impregnated zeolite Y as highly active and stable heterogeneous Fenton-like catalyst for degradation of Congo red dye. *Sep. Purif. Technol.* **2016**, *170*, 321–336. [[CrossRef](#)]
22. Viegas, R.M.C.; Mestre, A.S.; Mesquita, E.; Campinas, M.; Andrade, M.A.; Carvalho, A.P.; Rosa, M.J. Assessing the applicability of a new carob waste-derived powdered activated carbon to control pharmaceutical compounds in wastewater treatment. *Sci. Total Environ.* **2020**, *743*, 140791. [[CrossRef](#)] [[PubMed](#)]
23. Liyanage, A.S.; Canaday, S.; Pittman, C.U., Jr.; Mlsna, T. Rapid remediation of pharmaceuticals from wastewater using magnetic Fe₃O₄/Douglas fir biochar adsorbents. *Chemosphere* **2020**, *258*, 127336. [[CrossRef](#)]
24. Liu, Y.-X.; Zhong, H.; Li, X.-R.; Bao, Z.-L.; Cheng, Z.-P.; Zhang, Y.-J.; Li, C.-X. Fabrication of attapulgite-based dual responsive composite hydrogel and its efficient adsorption for methyl violet. *Environ. Technol.* **2020**. [[CrossRef](#)]
25. Zhang, T.; Nan, Z.-R. Decolorization of Methylene Blue and Congo Red by attapulgite-based heterogeneous Fenton catalyst. *Desalination Water Treat.* **2016**, *57*, 4633–4640. [[CrossRef](#)]
26. He, Y.; Sun, X.; Zhang, P.; Wang, F.; Zhao, Z.; He, C. Cd(II) adsorption from aqueous solutions using modified attapulgite. *Res. Chem. Intermed.* **2020**, *46*, 4897–4908. [[CrossRef](#)]
27. Guo, H.J.; Li, Q.L.; Zhang, H.R.; Peng, F.; Xiong, L.; Yao, S.M.; Huang, C.; Chen, X.D. CO₂ hydrogenation over acid-activated Attapulgite/Ce_{0.75}Zr_{0.25}O₂ nanocomposite supported Cu-ZnO based catalysts. *Mol. Catal.* **2019**, *476*, 14. [[CrossRef](#)]
28. Eslami, H.; Ehrampoush, M.H.; Esmaeili, A.; Ebrahimi, A.A.; Ghaneian, M.T.; Falahzadeh, H.; Salmani, M.H. Synthesis of mesoporous Fe-Mn bimetal oxide nanocomposite by aeration co-precipitation method: Physicochemical, structural, and optical properties. *Mater. Chem. Phys.* **2019**, *224*, 65–72. [[CrossRef](#)]
29. Association, C.; Washington, D. APHA: Standard methods for the examination of water and wastewater. American. *Phys. Educ. Rev.* **1995**, *24*, 481–486.
30. Ma, C.; Yuan, P.; Jia, S.; Liu, Y.; Zhang, X.; Hou, S.; Zhang, H.; He, Z. Catalytic micro-ozonation by Fe₃O₄ nanoparticles @ cow-dung ash for advanced treatment of biologically pre-treated leachate. *Waste Manag.* **2019**, *83*, 23–32. [[CrossRef](#)]
31. Li, Z.; Xin, Y.; Zhang, Z.; Wu, H.; Wang, P. Rational design of binder-free noble metal/metal oxide arrays with nanocauliflower structure for wide linear range nonenzymatic glucose detection. *Sci. Rep.* **2015**, *5*, 10617. [[CrossRef](#)] [[PubMed](#)]
32. Zhou, C.; Xu, L.; Song, J.; Xing, R.; Xu, S.; Liu, D.; Song, H. Ultrasensitive non-enzymatic glucose sensor based on three-dimensional network of ZnO-CuO hierarchical nanocomposites by electrospinning. *Sci. Rep.* **2014**, *4*, 7382. [[CrossRef](#)] [[PubMed](#)]
33. Guo, H.; Li, Q.; Zhang, H.; Xiong, L.; Peng, F.; Yao, S.; Chen, X. Attapulgite supported Cu-Fe-Co based catalyst combination system for CO hydrogenation to lower alcohols. *J. Fuel Chem. Technol.* **2019**, *47*, 1346–1356. [[CrossRef](#)]
34. Moradi, S.; Sobhgol, S.A.; Hayati, F.; Isari, A.A.; Kakavandi, B.; Bashardoust, P.; Anvaripour, B. Performance and reaction mechanism of MgO/ZnO/Graphene ternary nanocomposite in coupling with LED and ultrasound waves for the degradation of sulfamethoxazole and pharmaceutical wastewater. *Sep. Purif. Technol.* **2020**, *251*, 117373. [[CrossRef](#)]
35. Mahouachi, L.; Rastogi, T.; Palm, W.U.; Ghorbel-Abid, I.; Ben Hassen Chehimi, D.; Kummerer, K. Natural clay as a sorbent to remove pharmaceutical micropollutants from wastewater. *Chemosphere* **2020**, *258*, 127213. [[CrossRef](#)]
36. Naumczyk, J.; Prokurat, I.; Marcinowski, P. Landfill Leachates Treatment by H₂O₂/UV, O₃/H₂O₂, Modified Fenton, and Modified Photo-Fenton Methods. *Int. J. Photoenergy* **2012**, *2012*, 1–9. [[CrossRef](#)]
37. Yazici Guvenc, S.; Varank, G. Degradation of refractory organics in concentrated leachate by the Fenton process: Central composite design for process optimization. *Front. Environ. Sci. Eng.* **2020**, *15*, 2. [[CrossRef](#)]
38. Liu, Y.; Yang, Z.; Wang, J. Fenton-like degradation of sulfamethoxazole in Cu₀/Zn₀-air system over a broad pH range: Performance, kinetics and mechanism. *Chem. Eng. J.* **2020**, *403*, 126320. [[CrossRef](#)]
39. Zhang, Q.; Peng, Y.; Deng, F.; Wang, M.; Chen, D. Porous Z-scheme MnO₂/Mn-modified alkalized g-C₃N₄ heterojunction with excellent Fenton-like photocatalytic activity for efficient degradation of pharmaceutical pollutants. *Sep. Purif. Technol.* **2020**, *246*, 116890. [[CrossRef](#)]
40. Ma, C.; He, Z.; Jia, S.; Zhang, X.; Hou, S. Treatment of stabilized landfill leachate by Fenton-like process using Fe₃O₄ particles decorated Zr-pillared bentonite. *Ecotoxicol. Environ. Saf.* **2018**, *161*, 489–496. [[CrossRef](#)]
41. Nguyen, T.T.; Le, G.H.; Le, C.H.; Nguyen, M.B.; Quan, T.T.T.; Pham, T.T.T.; Vu, T.A. Atomic implantation synthesis of Fe-Cu/SBA-15 nanocomposite as a heterogeneous Fenton-like catalyst for enhanced degradation of DDT. *Mater. Res. Express* **2018**, *5*, 115005. [[CrossRef](#)]
42. Lou, Z.; Zhou, Z.; Zhang, W.; Zhang, X.; Hu, X.; Liu, P.; Zhang, H. Magnetized bentonite by Fe₃O₄ nanoparticles treated as adsorbent for methylene blue removal from aqueous solution: Synthesis, characterization, mechanism, kinetics and regeneration. *J. Taiwan Inst. Chem. Eng.* **2015**, *49*, 199–205. [[CrossRef](#)]

43. Kasiri, M.; Khataee, A. Photooxidative decolorization of two organic dyes with different chemical structures by UV/H₂O₂ process: Experimental design. *Desalination* **2011**, *270*, 151–159. [[CrossRef](#)]
44. Chen, W.; Westerhoff, P.; Leenheer, J.A.; Booksh, K. Fluorescence excitation-emission matrix regional integration to quantify spectra for dissolved organic matter. *Environ. Sci. Technol.* **2003**, *37*, 5701–5710. [[CrossRef](#)] [[PubMed](#)]
45. Wang, X.-T.; Li, Y.; Zhang, X.-Q.; Li, J.-F.; Luo, Y.-N.; Wang, C.-W. Fabrication of a magnetically separable Cu₂ZnSnS₄/ZnFe₂O₄ p-n heterostructured nano-photocatalyst for synergistic enhancement of photocatalytic activity combining with photo-Fenton reaction. *Appl. Surf. Sci.* **2019**, *479*, 86–95. [[CrossRef](#)]
46. Chen, T.; Zhu, Z.; Zhang, H.; Shen, X.; Qiu, Y.; Yin, D. Enhanced Removal of Veterinary Antibiotic Florfenicol by a Cu-Based Fenton-like Catalyst with Wide pH Adaptability and High Efficiency. *ACS Omega* **2019**, *4*, 1982–1994. [[CrossRef](#)]
47. Abbasi Asl, E.; Haghighi, M.; Talati, A. Enhanced simulated sunlight-driven magnetic MgAl₂O₄-AC nanophotocatalyst for efficient degradation of organic dyes. *Sep. Purif. Technol.* **2020**, *251*, 117003. [[CrossRef](#)]
48. Diao, Y.; Yan, Z.; Guo, M.; Wang, X. Magnetic multi-metal co-doped magnesium ferrite nanoparticles: An efficient visible light-assisted heterogeneous Fenton-like catalyst synthesized from saprolite laterite ore. *J. Hazard. Mater.* **2018**, *344*, 829–838. [[CrossRef](#)]
49. Lv, X.; Ma, Y.; Li, Y.; Yang, Q. Heterogeneous Fenton-Like Catalytic Degradation of 2,4-Dichlorophenoxyacetic Acid by Nano-Scale Zero-Valent Iron Assembled on Magnetite Nanoparticles. *Water* **2020**, *12*, 2909. [[CrossRef](#)]
50. di Luca, C.; Massa, P.; Grau, J.M.; Marchetti, S.G.; Fenoglio, R.; Haure, P. Highly dispersed Fe³⁺-Al₂O₃ for the Fenton-like oxidation of phenol in a continuous up-flow fixed bed reactor. Enhancing catalyst stability through operating conditions. *Appl. Catal. B Environ.* **2018**, *237*, 1110–1123. [[CrossRef](#)]